Hydrolysis of 1,8- and 2,3-naphthalic† anhydrides and the mechanism of cyclization of 1,8-naphthalic acid in aqueous solutions‡

Teresa C. Barros,§[a] Santiago Yunes,[b] Guilherme Menegon,[a] Faruk Nome,[b] Hernan Chaimovich,[a] Mario J. Politi,[a] Luis G. Dias[a] and Iolanda M. Cuccovia *[a]

[a] *Departamento de Bioquímica, Instituto de Química, Universidade de São Paulo, Brazil*
[b] *Departamento de Química, Universidade Federal de Santa Catarina, Florianópolis, Brazil*

Received (in Cambridge, UK) 4th May 2001, Accepted 21st September 2001
First published as an Advance Article on the web 24th October 2001

Naphthalene-1,8-dicarboxylic acid, 1,8-Acid, cyclizes spontaneously in acidic aqueous solution to naphthalene-1,8-dicarboxylic anhydride, 1,8-An, and here we present an *ab initio* study of the reaction pathway. The effect of pH on the hydrolysis of 1,8-An was analysed and compared with the hydrolysis of naphthalene-2, 3-dicarboxylic anhydride, 2,3-An, to naphthalene-2,3-dicarboxylic acid, 2,3-Acid. The values of the pK_a's of 1,8-Acid and 2,3-Acid were *ca.* 3.5 and 3.0, for monoanion formation, pK_{a1}, and 5.5 and 5.0 for dianion formation, pK_{a2}, respectively. Fluorimetric titration demonstrated that the diprotonated 2,3-Acid, AH_2, was further protonated to yield AH_3^+. The pH–rate constant profile for 2,3-An hydrolysis showed a water reaction between pH's 1.0 and 6.0 and a base catalysed hydrolysis above pH 7.0. Under no condition was 2,3-An formed from 2,3-Acid. The pH dependent decomposition kinetics of 1,8-An is complex and, below pH 6.0, the pH–rate constant profile was fitted by assuming that both AH_2 and AH_3^+ are in equilibrium with 1,8-An. The values of the equilibrium constants for 1,8-An formation from AH_2 and AH_3^+ were *ca.* 4 and 100 in dilute and concentrated acid, respectively. *Ab initio* calculations for a possible reaction pathway connecting the undissociated 1,8-Acid to 1,8-An show a transition state where an intramolecular proton transfer is concerted with oxygen alignment towards the carbonyl centre. The planar intermediate is then dehydrated yielding a complex between water and 1,8-An.

Introduction

Carboxylic anhydrides hydrolyse in water and the reaction can be acid or base catalysed.[1–6] In aqueous solution even monocarboxylic acids readily equilibrate with the corresponding anhydride, although the equilibrium strongly favours the acid.[7,8]

The equilibrium constants for anhydride formation, $K_E = k_1/k_{-1}$ = [anhydride]/[dicarboxylic acid] [eqn. (1)], have been determined in several cases.[9–12]

$$\text{Dicarboxylic Acid} \underset{k_{-1}}{\overset{k_1}{\rightleftharpoons}} \text{Anhydride} + H_2O \qquad (1)$$

The values of K_E vary from 10^{-7} to 25 depending on the structure of the diacid. The unionized acid is the kinetically active species in anhydride formation.[12]

The hydrolysis of cyclic anhydrides has been studied in aqueous media and in water–solvent mixtures. There are several correlations between rates and nature of the acid, size and configuration of the anhydride ring for both mono- and bi-cyclic anhydrides.[13]

The model system most extensively used to analyse particular aspects of enzymatic catalysis covalently incorporate reactants into the same molecule, modelling bimolecular reactions in an intramolecular system.[2] Relative accelerations, obtained by comparisons of the second and first order rate constants can reach values as large as 10^{13} in model systems based upon naphthalic acid derivatives.[3] Due the importance of modelling peptide cleavage by using simple organic compounds we studied the hydrolysis of 2,3- and *N*-butyl-1,8-naphthalimides.[4] Alkaline hydrolysis of *N*-butyl-1,8-naphthalimide includes ring opening yielding naphthalamic acid which, at low pH, cyclizes to the naphthalene-1,8-dicarboxylic anhydride, 1,8-An.[4] The alkaline hydrolysis of *N*-butyl-2,3-naphthalimide, however, yields naphthalamic acid, which does not cyclize in acid.[4] The analysis of imide hydrolysis in this system would be simplified by understanding the mechanism of 1,8-An formation from naphthalene-1,8-dicarboxylic acid, 1,8-Acid.[4,5]

Here we present the study of the equilibrium reaction between naphthalene-1,8-dicarboxylic acid and its anhydride in aqueous acid, the alkaline hydrolysis of 1,8-An, and compare these data with the hydrolysis of naphthalene-2,3-dicarboxylic anhydride (Scheme 1).

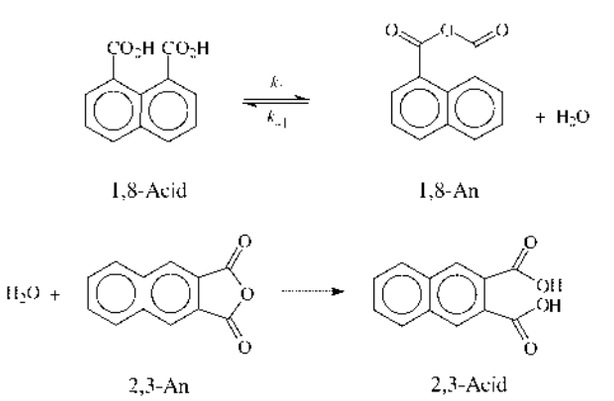

Scheme 1

† The IUPAC name for naphthalic acid is napthalenedicarboxylic acid.
‡ Electronic supplementary information (ESI) available: tables containing the values of the rate constants. See http://www.rsc.org/suppdata/p2/b1/b104148g/
§ *Present address*: Instituto de Ciências da Saúde, Universidade Paulista, UNIP, Bauru, São Paulo, Brazil.

 DOI: 10.1039/b104148g

Experimental

Materials

Naphthalene-1,8-dicarboxylic anhydride, 1,8-An (Aldrich), was purified by sublimation. Naphthalene-2,3-dicarboxylic anhydride, 2,3-An, was synthesised and purified using standard procedures.[14] Naphthalene-2,3-dicarboxylic acid, 2,3-Acid (Aldrich), was used as received. Naphthalene-1,8-dicarboxylic acid, 1,8-Acid, was prepared by adding 0.03 M NaOH to a water suspension of 1,8-An (0.01 M) and maintaining the sample at 50 °C for 5 h. At the end of the reaction absorbance measurements (at 343 nm) assured total absence of the anhydride (see below).

All reagents were PA grade or better and organic solvents were distilled. All aqueous solutions and buffers were prepared in freshly glass-bi-distilled water.

Methods

Absorbance spectra (UV–visible) and kinetic measurements were obtained on a Hewlett-Packard HP8452A spectrophotometer equipped with a thermostatted water-jacketed cell holder (Microquímica MQBTZ99-20), or a Beckman DU-7 spectrophotometer equipped with a Peltier block. Fluorescence measurements were made on a Hitachi F-2000 spectrofluorometer. pH was measured with a Beckman model Φ71 pH meter. The electrode was calibrated against standard buffers, in a thermostatted stirred vessel, at the appropriate temperature (±0.1 °C). The pH of the buffers was adjusted with NaOH. Titration of the 2,3-Acid and 1,8-Acid were made on a Radiometer PHM 82 Standard pH Meter equipped with a glass electrode calibrated with standard buffers at 30 °C.

Kinetics

The kinetics of hydrolysis and cyclization of the substrates were followed at 343 nm for 1,8-An ($\varepsilon = 12900\ M^{-1}\ cm^{-1}$) and 365 nm for 2,3-An ($\varepsilon = 3600\ M^{-1}\ cm^{-1}$) in a quartz cell of 1 cm optical path. The reaction was initiated by adding 20 μL of a stock solution of the substrates prepared in acetonitrile to 2.0 ml of buffer. The final concentration of substrate was 1.0×10^{-5} M for the reactions performed at 30 °C and 1.7×10^{-5} M at 50 °C. The buffers used were borate (pH 9.0 to 10.0), phosphate (pH 6.4 to 8.0), citrate (pH 2.2 to 6.0) and HCl for pH's lower than 2.0, where the H_0 scale was used.[15] The buffer concentrations are detailed in the tables and figure legends. The absorbance values were stored directly on a microcomputer and analysed using the HP 8452 kinetics software. Data analysis demonstrated first order behaviour for, at least, 4–5 half-lives. Reported rate constants are averages of, at least, three independent determinations differing by no more than 5%.

pK_a determinations

All determinations were made at 30 °C.

Potentiometric titrations. The 2,3-Acid was titrated with HCl using 50 mL of a 0.001 M solution of 2,3-Acid made alkaline with NaOH to pH 11.0, with or without NaCl, under a N_2 atmosphere. Titrating HCl (0.0667 M) was added to the solution with a Hamilton microsyringe. 1,8-Acid was titrated potentiometrically with HCl (0.0667 M) under N_2 using an aliquot of 5.0 mL of a 0.01 M solution of 1,8-Acid (pH 12.0) diluted to 50 mL. The initial pH in this solution is near 11.0. Since the pK_{a2} of 1,8-Acid is near 5.5, and at this pH the 1,8-Acid does not cyclize (see below), it is not necessary to consider the anhydride–acid equilibrium.

The potentiometric titration of 1,8-Acid at pH's lower than 4.0 were completed in *ca.* 15 min. On this time scale, the maximum calculated amount of 1,8-An formed upon cyclization of 1,8-Acid is 15%. Hence in this pH region the anhydride–acid equilibrium needs to be considered.

Spectrometric titrations. The pK_{a1} and pK_{a2} of 2,3-Acid (Scheme 2) were determined from the absorbance (255 nm)

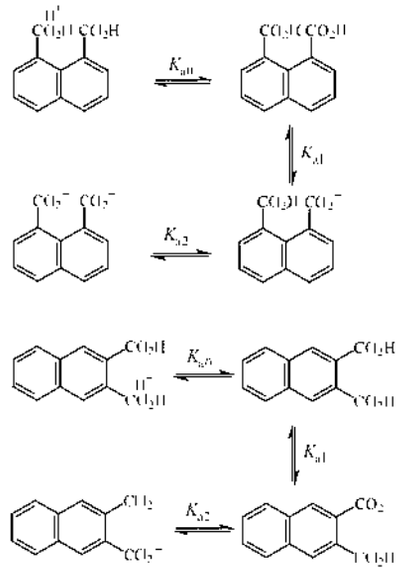

Scheme 2

measured at several pH's, by adding 0.025 mL of 1×10^{-3} M methanolic solution of the 2,3-Acid to 2.5 mL of 0.10 M buffer. The buffers used were borate, phosphate and citrate from pH 9 to 2.5 and HCl at lower pH's.

The values of pK_{a0}, pK_{a1} and pK_{a2} of 2,3-Acid were determined from the variation of the uncorrected fluorescence emission intensities at 378 nm using the excitation wavelength fixed at 300 nm. pK_{a1} of 1,8-Acid was determined using emission intensities at 420 nm and excitation wavelength at 300 nm. Excitation and emission slits were fixed to a 10 nm bandpass width. Fluorescence rectangular quartz cells of 1 cm optical pathlength were used with a 90° excitation–emission geometry. A methanolic solution, 0.025 mL, of 2,3-Acid 1×10^{-3} M was added to 2.5 mL of buffer giving a final concentration 1×10^{-5} M. For 1,8-Acid, a 1×10^{-3} M solution in NaOH pH 11 was used.

The values of pK_{a1} and pK_{a2} of 1,8-Acid (Scheme 2) were obtained by absorbance measurements (320 nm) at several pH's in 1.0 cm optical pathlength quartz cells. 1,8-Acid (0.05 mL, 0.01 M) was added to 2.5 mL of 0.10 M buffer yielding a final concentration of 2×10^{-4} M of 1,8-Acid.

Since absorbance or fluorescence values were obtained within *ca.* 20 seconds of 1,8-Acid addition to the buffered solution no correction on the pK_a values regarding the anhydride–acid equilibrium was necessary.

Computational procedures

***Ab initio* calculations.** The potential energy surface for the formation of 1,8-An was studied by *ab initio* quantum chemical methods. The gas-phase geometries of reactant, products, intermediate and transition states were fully optimised at the Hartree–Fock (HF) level of theory using the standard 6-31G* basis set. Electron correlation energy was included by single-point calculations at second-order Møller–Plesset perturbation theory (MP2), using the same basis set. The characteristics of all stationary points were evaluated by calculations of vibration harmonic frequencies at the HF/6-31G* level. Vibrational harmonic frequencies were obtained from second-order analytical energy derivatives. Assuming ideal behaviour, partition functions (translational, rotational, vibrational and electronic) and thermodynamic properties (referring to the standard state of

Table 1 pK_a's of naphthalic acids and phthalic acids

Compound	Method	Salt or buffer	pK_{a0}	pK_{a1}	pK_{a2}
1,8-Acid	Potentiometric	0		3.63	5.53
	Potentiometric	NaCl 0.02 M		3.52	5.38
	Potentiometric	NaCl 0.10 M		3.54	5.44
	Spectrophotometric	Buffer 0.1 M		3.50	5.40
	Fluorescence	Buffer 0.02 M		3.56	
	Fluorescence	Buffer 0.05 M		3.49	
2,3-Acid	Potentiometric	0		3.27	5.28
	Potentiometric	NaCl 0.02 M		3.33	5.09
	Potentiometric	NaCl 0.10 M		3.05	5.00
	Spectrophotometric	Buffer 0.1 M		2.80	5.00
	Fluorescence	Buffer 0.1 M	−0.30	2.80	4.90
o-Phthalic acid [a]				2.89	5.51
m-Phthalic acid [a]				3.54	4.60
p-Phthalic acid [a]				3.51	4.82

[a] Ref. 28.

1 mol L^{-1} and 298 K) were calculated by employing standard statistical mechanical theory.[16] Low frequency modes were subtracted from enthalpic and entropic contributions.

Reaction coordinate points were determined using the intrinsic reaction coordinate (IRC) approach, also at the HF/6-31G* level, using the method of Gonzales and Schlegel.[17,18] Solvation free energies (related to the transfer of the solute molecule from the 1 mol L^{-1} vapour to 1 mol L^{-1} aqueous solution at 298 K) were calculated at the MP2/6-31G* level by using the polarized-continuum model (PCM) and standard atomic radii, at the gas-phase determined geometries.[19,20]

Addition of the energetic and entropic contributions to the MP2/6-31G*//HF/6-31G* electronic energies gave the gas-phase free energies. Aqueous-phase free energies were obtained from further addition of solvation (PCM) contributions.

Results

The values of pK_{a1} and pK_{a2}, of 1,8-Acid and 2,3-Acid (Scheme 2), calculated from potentiometric titration curves,[21] with and without NaCl are presented in Table 1. NaCl produced a moderate decrease in the pK_a's of both diacids (Table 1).

The values of pK_{a1} and pK_{a2} of 2,3-Acid and 1,8-Acid were also determined by UV spectra (Fig. 1). The data in Figs. 1A and 1B were fitted using eqn. (2). Abs_T and C_T are the absorbance and the total concentration of the diacid, and pK_{a1} and pK_{a2} refer to the dissociation constants of the diacid, K_{a1} and K_{a2} (Scheme 3), as defined by eqns. (3) and (4).

$$Abs_T = C_T \frac{(\varepsilon_A \times 10^{(pH-pK_{a2})} \times 10^{(pH-pK_{a1})} + \varepsilon_{AH} \times 10^{(pH-pK_{a1})} + \varepsilon_{AH_2})}{(1 + 10^{(pH-pK_{a1})} + 10^{(pH-pK_{a1})} \times 10^{(pH-pK_{a2})})} \quad (2)$$

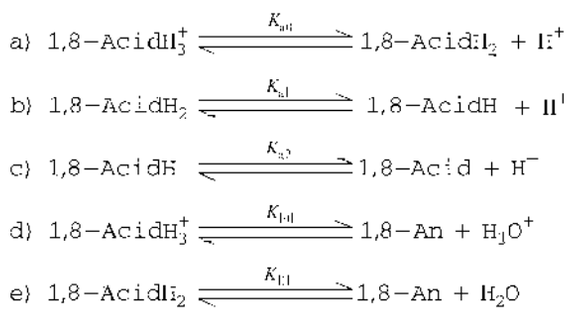

Scheme 3

$$K_{a1} = \frac{[AH][H^+]}{[AH_2]} \quad (3)$$

$$K_{a2} = \frac{[A][H^+]}{[AH]} \quad (4)$$

The values of the molar extinction coefficients ε_{AH_2}, ε_{AH} and ε_A, corresponding to diprotonated, AH_2, monoprotonated, AH, and dianionic species, A, respectively, are presented in the legend of Fig. 1.

The values of pK_{a1} and pK_{a2} of 1,8-Acid and 2,3-Acid, estimated by spectral measurements (Table 1) are, within the experimental error, similar to those determined by potentiometric titration and in the same range of pK_a's of derivatives of phthalic acid, Table 1.[22]

Photophysical properties of 1,8-Acid and 2,3-Acid have been described.[23] pK_a values of both 1,8-Acid and 2,3-Acid were determined by changes in fluorescence emission yields with pH and are included in Table 1.

Since 2,3-Acid does not cyclize even at very low pH, the fluorescence emission of 2,3-Acid was determined at high acidities and another pK_a was apparent (Fig. 1C). The pK_a in the H_0 region, pK_{a0}, was attributed to the protonation of 2,3-AcidH_2, AH_2, leading to 2,3-AcidH_3^+, AH_3^+ (Scheme 3), as described in eqn. (5).

$$K_{a0} = \frac{[AH_2][H^+]}{[AH_3^+]} \quad (5)$$

The fluorescence decrease at high HCl concentration was not due to quenching of the AH_2 fluorescence by chloride ion, but rather a significant decrease in quantum yield due to the formation of AH_3^+ species.[23] The fluorescence of the 2,3-Acid in 5.0 M HCl decreases 95% compared with that in pH 2.0, while the addition of 5.0 M NaCl to 2,3-Acid at pH 2.0 leads to only a 30% decrease in the fluorescence intensity.

The values of the relative fluorescence intensity, *F*, *versus* pH were adjusted using eqn. (6) where C_T is the total 2,3-Acid concentration, ϕAH_3, ϕAH_2, ϕAH, and ϕA are adjustable parameters (presented in the legend of Fig. 1C) proportional to the molar absorption coefficient at the excitation wavelength and the emission yield for the 2,3-Acid species.

The calculated values of the three pK_a's of 2,3-Acid are presented in Table 1.

The hydrolysis of 2,3-An was studied over a wide pH range. The observed rate constant, k_ψ, for 2,3-An hydrolysis does not

$$F = C_T \frac{(\phi AH_3 + \phi AH_2 \times 10^{(pH-pK_{a0})} + \phi AH \times 10^{(pH-pK_{a1})} \times 10^{(pH-pK_{a0})} + \phi A \times 10^{(pH-pK_{a2})} \times 10^{(pH-pK_{a1})} \times 10^{(pH-pK_{a0})})}{(1 + 10^{(pH-pK_{a0})} + 10^{(pH-pK_{a0})} \times 10^{(pH-pK_{a1})} + 10^{(pH-pK_{a0})} \times 10^{(pH-pK_{a1})} \times 10^{(pH-pK_{a0})})} \quad (6)$$

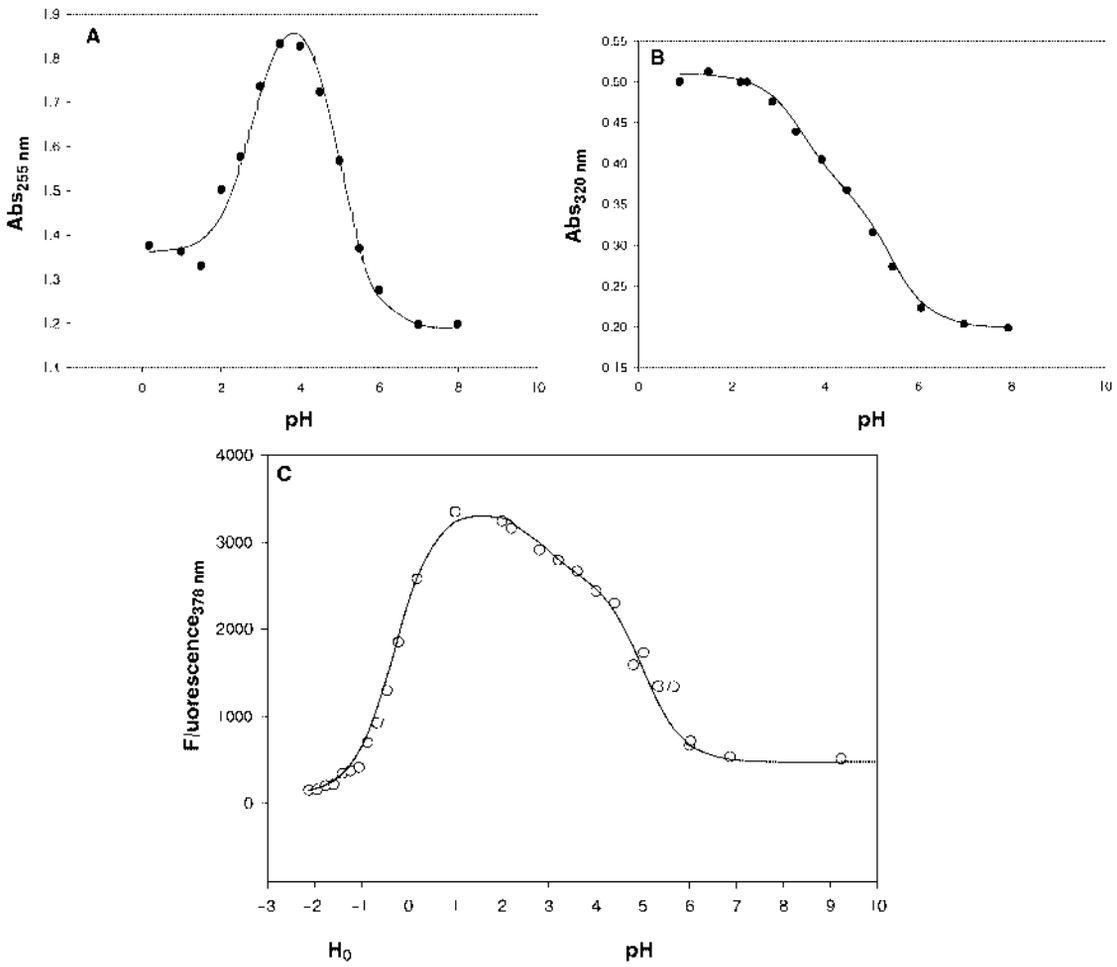

Fig. 1 pH effect on the absorbance or fluorescence of: (A) 2,3-Acid: the concentration of 2,3-Acid was 1×10^{-4} M and the solid line was calculated using $\varepsilon_A = 1190$ M^{-1} cm^{-1}; $\varepsilon_{AH} = 1950$ M^{-1} cm^{-1}; $\varepsilon_{AH_2} = 1360$ M^{-1} cm^{-1} in eqn. (2). (B) 1,8-Acid: the concentration of 1,8-Acid was 2×10^{-4} M and the solid line was calculated using eqn. (2) and the following parameters: $\varepsilon_A = 1000$ M^{-1} cm^{-1}; $\varepsilon_{AH} = 1850$ M^{-1} cm^{-1}; $\varepsilon_{AH_2} = 2500$ M^{-1} cm^{-1}. (C) 2,3-Acid: the sample was excited at 300 nm and the fluorescence measured at 378 nm. The solid line was calculated using eqn. (6) and $\phi AH_3 = 100$; $\phi AH_2 = 3400$; $\phi AH = 2600$ and $\phi A = 475$. The concentration of 2,3-Acid was 1×10^{-5} M, buffers 0.1 M and the temperature 30 °C.

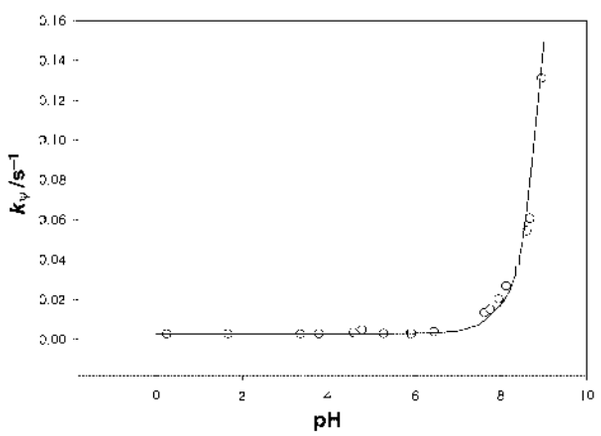

Fig. 2 pH effect on observed rate constant of hydrolysis of 2,3-An at 30 °C. The line was obtained using eqn. (7) and the parameters used are in Table 2.

Table 2 Rate and equilibrium constants for the reactions of hydrolysis of 2,3-An and 1,8-An[a]

	1,8-An		2,3-An
Parameters	30 °C	50 °C	30 °C
k_H/M^{-1} s^{-1}	1.2×10^{-4}	1.13×10^{-3}	
k_{OH}/M^{-1} s^{-1}	1.3×10^{3}	3.20×10^{3}	9.9×10^{3}
k_{-1}/s^{-1}; k_{-2}/s^{-1}	5.0×10^{-5}	3.30×10^{-4}	2.8×10^{-3}
k_2/s^{-1}	8.0×10^{-4}	3.90×10^{-3}	
k_1/s^{-1}	1.5×10^{-4}	1.35×10^{-3}	
K_{a0} (pK_0)	2.45 (−0.39)	2.45 (−0.39)	
K_{a1} (pK_{a1})	2.51×10^{-4} (3.6)	3.55×10^{-4} (3.45)	
K_{a2} (pK_{a2})	3.16×10^{-6} (5.5)		
K_{E0}		115.5	
K_{E1}	3.0	4.25	

[a] Values obtained from adjusting experimental data to kinetic and equilibrium equations (see text).

vary from pH 0.0 to 7.0 (Fig. 2), increasing sharply with pH in alkali. The slope of the linear log k_ψ–pH function was 1.0 above pH 7.0 (not shown) and the k_ψ–pH pattern can be attributed to the water attack on 2,3-An up to pH 7.0 and OH^- catalysed hydrolysis in alkali.[24,25] The data of Fig. 2 were adjusted using eqn. (7), where k_{-1} is the first order rate constant for water attack on anhydride and k_{OH} is the second order rate constant for OH^- attack. The values of the rate constants are presented in Table 2.

$$k_\psi = k_{-1} + k_{OH}[OH] \quad (7)$$

The spectra of 2,3-Acid, product of the hydrolysis of 2,3-An, remained unchanged, even for 5 days at 50 °C in HCl 5.0 M (not shown), implying that if any 2,3-An is formed under these conditions, the equilibrium strongly favours the 2,3-Acid.

The k_ψ–pH dependence for 1,8-An hydrolysis is complex, consisting of an acid catalysed region at pH's lower than 1.0, a well defined plateau between pH 1.2 and 2.4, a pH dependent

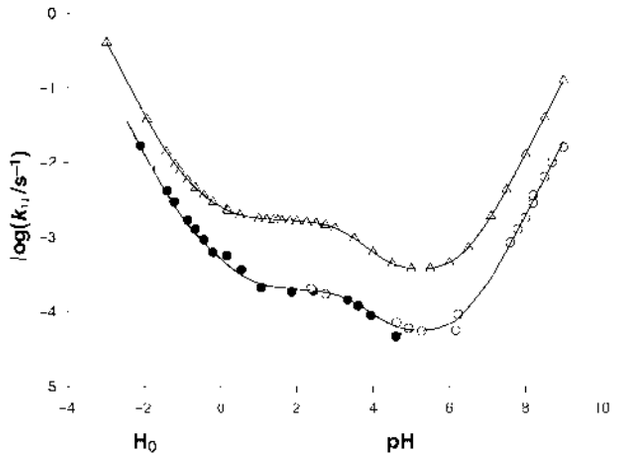

Fig. 3 Observed rate constant for the hydrolysis of 1,8-An and attainment of equilibrium between 1,8-An and 1,8-Acid as a function of pH–H_0. At 30 °C (0.02 M buffer) the rate constants were obtained starting with: (a) 1,8-An for hydrolysis (above pH 6.0) and equilibrium (below pH 6.0) (O) and (b) 1,8-Acid (●). At 50 °C (0.1 M buffer) rate constants for both hydrolysis (above pH 6.0) and equilibrium attainment were obtained starting the reaction with 1,8-An (Δ). The pH scale at $[H^+] > 1.0$ M is given in H_0. The lines were obtained using eqns. (18), (23) and (25) and the parameters used are in Table 2.

region between pH 2.5 and 4.5, a water catalysed region and a OH^- catalysed reaction above pH 7.0 (Fig. 3).

Below pH 4.5 the values of k_ψ increase to a plateau with an apparent pK, pK_{ap}, near 4.0 at 30 and 50 °C. The values for k_ψ, below pH 4.5, were the same whether the reaction was started by addition of 1,8-Acid or 1,8-An (Fig. 3), demonstrating that k_ψ, in this pH region, is related to the rate of diacid–anhydride equilibrium attainment.

The quantitative analysis of the kinetic data presented in Fig. 3 required the analysis of the diacid–anhydride equilibrium. The marked spectral difference between 1,8-Acid and 1,8-An, as observed upon 1,8-An hydrolysis at pH 7.5 (Fig. 4A), allowed the determination of the anhydride concentration at equilibrium as a function of pH at 340 nm where only the anhydride absorbs. The absorbance at equilibrium, A_{ET}, was determined at 50 °C (Fig. 4B).

The final absorbance obtained using 1,8-An as substrate at pH's higher than 6.0 does not change with pH, consistent with near quantitative hydrolysis of 1,8-An to 1,8-Acid in this pH range. Furthermore no absorbance change is detected at pH higher than 7.0 when 1,8-Acid is used as substrate, strongly suggesting that the dissociated ionic forms of the diacid do not cyclize.

At pH's lower than 4.5 the equilibrium absorbance increases becoming constant between pH 2.0 and 0. As the acid concentration increases the absorbance increases again reaching a value consistent with near quantitative anhydride formation (Fig. 4B). As expected, the values of A_{ET} at several pH's were identical using either 1,8-Acid or 1,8-An to initiate the reaction.

From data of Fig. 4B it can be supposed that there are two equilibrium phenomena, involving differently protonated species, one between pH 4.5 and 0.0 and another below pH 0.0. One of the simplest forms to rationalise these results follows. Between pH 0 and 4.5 equilibrium is established, as described for several related systems,[12] between the anhydride and AH_2. At $[H^+] > 1.0$ M equilibrium is established between the anhydride and the protonated form of 1,8-AcidH_2, 1,8-AcidH_3^+ (Scheme 3).

In fact protonation of both cyclic anhydrides and dicarboxylic acids were proposed decades ago.[26,27] The variation of A_{ET} with pH was analysed by assuming that formation of 1,8-An can occur from 1,8-AcidH_3^+ and from the neutral 1,8-AcidH_2 and can be described by the equilibrium constants K_{E0} and K_{E1}, respectively (Scheme 3).

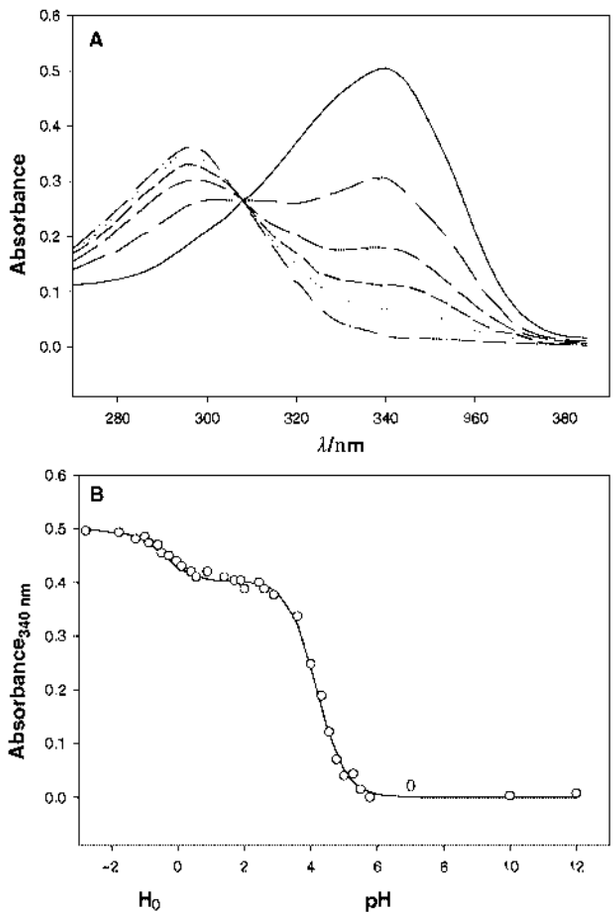

Fig. 4 (A) Hydrolysis of 1,8-An followed by UV spectra at pH 7.5, 50 °C. Spectra were obtained after intervals of 45 seconds, (——) initial spectrum of 1,8-An and (—•—•—) final spectra of 1,8-Acid. (B) Absorbances at 340 nm, after attainment of equilibrium between 1,8-An and 1,8-Acid at 50 °C, HCl pH 2.5. Scale of pH at values lower than zero is in H_0. The solid line was obtained using eqn. (16).

Here, as previously shown in related systems, the monoprotonated form of 1,8-Acid, AH, does not cyclize to the anhydride.[9,12]

Considering, as described repeatedly,[2] that $[H_2O]$ is constant, K_{E0} and K_{E1} can be defined as shown in eqns. (8) and (9).

$$K_{E0} = \frac{k_2}{k_{-2}} = \frac{[An]}{[AH_3^+]} \quad (8)$$

$$K_{E1} = \frac{k_1}{k_{-1}} = \frac{[An]}{[AH_2]} \quad (9)$$

The absorbance at the equilibrium at each pH, A_{ET}, (Fig. 4B) was related to eqns. (8) and (9) and Scheme 3 as follows. A_T, is taken as the absorbance corresponding to quantitative anhydride formation. 1,8-Acid does not absorb at 340 nm; hence, at any pH absorbance is related only to anhydride concentration. The absorbance contribution from the anhydride produced from AH_3^+, in the absence of any other ionic species, is defined as A_{E1}, and that from AH_2 as A_{E2}. Since the ratio of 1,8-AcidH_2 and 1,8-AcidH_3^+ changes with acidity, the value of A_{ET} will be the sum of the molar fraction of 1,8-AcidH_3^+ (α) and 1,8-AcidH_2 (β) multiplied by A_{E1} and A_{E2}, respectively [eqn. (10)].

$$A_{ET} = \alpha A_{E1} + \beta A_{E2} \quad (10)$$

Eqn. (13) can be derived, given the definitions in eqns. (11) and (12), where the subscript E refers to equilibrium concentrations.

Table 3 Thermodynamic parameters of the equilibrium between 1,8-Acid[a] and 1,8-An and comparison with the same reaction using DMPAcid and DMPAn

Reagent	Product	ΔH/kJ mol^{-1}	ΔS/J mol^{-1} K^{-1}	ΔG^b/kJ mol^{-1}
1,8-Acid	1,8-An	10.1 ± 1.9	42.8 ± 5.8	−3.72 × 0.02
DMPAcid	DMPAn	16.51[c]	37.8[c]	4.3[b,c]

[a] Thermodynamic parameters at pH 2.5 for the reaction of cyclization of 1,8-Acid to 1,8-An were calculated from measured equilibrium constants at several temperatures using: $\Delta G = -RT\ln K_{eq}$; $\ln K_{eq} = \Delta S/R - (\Delta H/R) \times 1/T$; $R = 8.317$ J K^{-1} mol^{-1}. [b] ΔG was calculated for K_{eq} at 50 °C. [c] The ΔG value for the cyclization reaction of DMPAcid to anhydride at 50 °C was calculated from literature data[11] for comparison.

$$A_{E1} = \frac{A_T}{\left(1 + \left(\frac{1 + K_{a0}/[H^+]}{K_{E0}}\right)\right)} \quad (11)$$

$$A_{E2} = \frac{A_T}{\left(1 + \left(\frac{1 + K_{a1}/[H^+]}{K_{E1}}\right)\right)} \quad (12)$$

$$[AH_2]_E = [AH_3^+]_T - [AH_3^+]_E \quad (13)$$

Using eqns. (8), (9) and (13), eqns. (14)–(16) can be derived.

$$\frac{[AH_3^+]_E}{[AH_3^+]_T} = \frac{K_{a0}}{(K_{a0} + [H^+])} = \alpha \quad (14)$$

$$\frac{[AH_2]_E}{[AH_2]_T} = \frac{[H^+]}{(K_{a1} + [H^+])} = \beta \quad (15)$$

The experimental A_{ET}–pH dependence (Fig. 4B) was analysed using eqn. (16) and the best fit values, at 50 °C, were $K_{a0} = 2.45$ (p$K_{a0} = -0.39$), $K_{a1} = 3.55 \times 10^{-4}$, (p$K_{a1} = 3.45$), $K_{E0} = 115.5$ and $K_{E1} = 4.25$ (Table 2). The value of pK_{a1} calculated from the fit of the equilibrium data with eqn. (16) is very similar to that determined by titration a 30 °C (Table 1). The value of pK_{a0} (Table 2) obtained by fitting the equilibrium data between 1,8-An and 1,8-Acid using eqn. (16) is identical to that determined for 2,3-Acid by fluorescence titration (Table 1).

$$A_{ET} = \frac{A_T}{\left(1 + \frac{[H^+]}{K_{a0}}\right)\left(1 + \frac{(1 + K_{a1}/[H^+])}{K_{E1}}\right)} + \frac{A_T}{\left(1 + \frac{K_{a0}}{[H^+]}\right)\left(1 + \frac{(1 + K_{a1}/[H^+])}{K_{E0}}\right)} \quad (16)$$

The effect of temperature on K_{E1} was determined at pH 2.5, where essentially all the 1,8-Acid is in the AH_2 form. The values of ΔS and ΔH, calculated from the linear plots of $\ln K_{E1}$ *vs.* $1/T$, are shown in Table 3.

After the determination of the equilibrium constants for anhydride formation and pK_a's of 1,8-Acid (Fig. 3) the pH effect on the rate constants of 1,8-An decomposition can be analysed quantitatively.

At pH's higher than 7, the predominant reaction is the alkaline hydrolysis of 1,8-An. The reaction rate, v, in this region and the observed rate constant, k_ψ, are given by eqns. (17) and (18), where k_{OH} is the second order rate constant for OH^-

$$v = k_\psi[1,8\text{-An}] \quad (17)$$

$$k_\psi = k_{OH}[OH^-] + k_{-1} \quad (18)$$

attack on the anhydride and k_{-1} is the rate constant of water attack on the anhydride.

The plot of log k_ψ *vs.* pH, from pH 7.0 to 9.0, was linear with a slope of 1.0 at 50 and 30 °C and the calculated value of k_{OH} is shown in Table 2. The pK_w values used for the calculation of $[OH^-]$ at 30 and 50 °C were 13.833 and 13.2617 respectively.[28] The value of k_{-1} was determined at the pH independent region, between pH 5.5 and 6.0, Table 2.

Between pH 1.0 and 5.0, where the concentration of anhydride at equilibrium is measurable, the observed rate constant reflects the kinetic process for attainment of equilibrium between the diacid and the anhydride. Assuming that AH_2 is the kinetically active species in this range of pH the reaction rate is given by eqn. (19) where k_1 is the rate constant for AH_2 cyclization.

$$\frac{d[An]}{dt} = -d\frac{[AH_2]}{dt} = k_1[AH_2] - k_{-1}[An] \quad (19)$$

In this pH range the total acid concentration, $[1,8\text{-Acid}]_T$, is given by eqn. (20).

$$[Acid]_T = [AH] + [AH_2] + [AH_3^+] \quad (20)$$

Using eqns. (3), (5) and (20), eqn. (21) can be derived.

$$[Acid]_T = [AH_2](1 + K_{a1}/[H^+] + [H^+]/K_{a0}) \quad (21)$$

Eqns. (19) and (21) give rise to eqn. (22) and k_ψ for equilibrium cyclization from AH_2, the predominant active species between pH 5 and 2, is given by eqn. (23).[9]

$$-d\frac{[AH_2]}{dt} = [Acid]_T\left(\frac{k_1}{(1 + K_{a1}/[H^+] + [H^+]/K_{a0})}\right) - k_{-1}[An] \quad (22)$$

$$k_\psi = \left(\frac{k_1}{(1 + K_{a1}/[H^+] + [H^+]/K_{a0})} + k_{-1}\right) \quad (23)$$

At pH's lower than 2.0 the ionic form AH_3^+ contributes to the equilibrium anhydride formation. The reaction in this acidity range can be characterised by the equilibrium between AH_3^+ and 1,8-An and an acid catalysed reaction, k_H, for the cyclization of AH_3^+ (see Fig. 3). The reaction rate is given by eqn. (24), where k_2 and k_{-2} are the rate constants for formation and decomposition of 1,8-An from AH_3^+, respectively.

$$v = k_H[H^+][AH_3^+] + k_2[AH_3^+] - k_{-2}[An] \quad (24)$$

The plot of k_ψ *vs.* a_{H^+}, at values of H_0 lower than −1, is linear and from the slope of the plot the value of k_H was obtained. From the pertinent acid–base dissociation equilibria it can be shown that eqn. (25) is true.

$$k_\psi = (k_H[H^+] + k_2)\left(\frac{[H^+]/K_{a0}}{1 + [H^+]/K_{a0} + K_{a1}/[H^+]}\right) + k_{-2} \quad (25)$$

The k_ψ *vs.* pH profiles of Fig. 3, at 30 and 50 °C, were adjusted using eqns. (18), (23) and (25). Between pH 1.0 and 5.0 the only adjustable parameter was k_1. Below pH 1.0 both k_2 and k_{-2} were varied to fit the experimental data to eqn. (25). As an

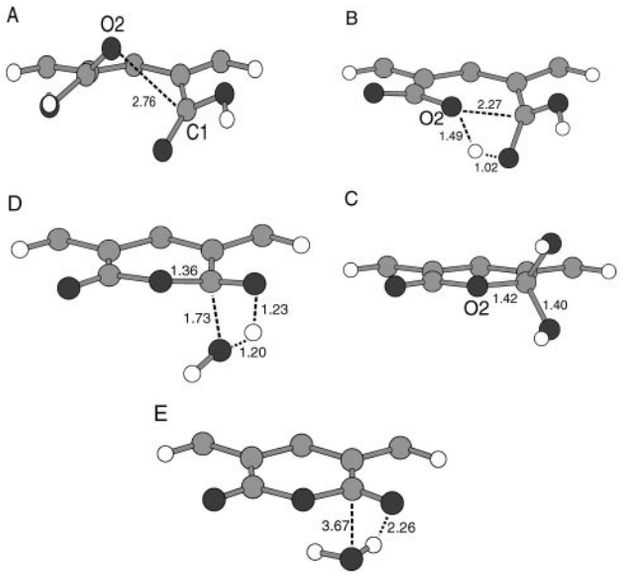

Fig. 5 Structure of the possible reactant A (1,8-Acid), transition states B and D, intermediate C and products E (1,8-An + H_2O) in the cyclization reaction. The naphthalic ring atoms are not shown for a better structure visualisation.

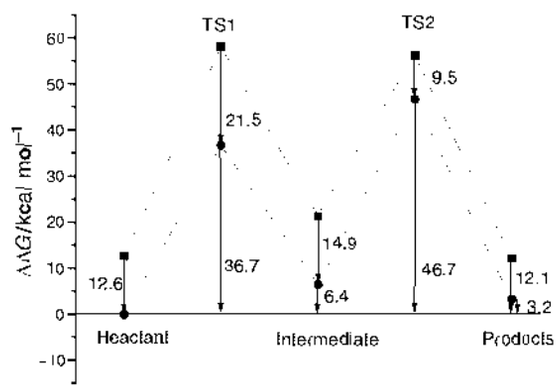

Fig. 6 Relative MP2/6-31G*//HF/6-31G* activation energies for the gas phase (■) and solution (●) for the cyclization reaction of 1,8-Acid.

initial estimate we assumed that $k_{-1} = k_{-2}$. The best fit values for the rate and equilibrium constants are presented in Table 2.

The study of the potential energy surface for the formation of 1,8-An from 1,8-Acid, AH_2 form, led us to the following reaction scheme: 1,8-Acid ⟶ TS1 ⟶ Intermediate ⟶ TS2 ⟶ 1,8-An + H_2O. The fully optimised structures are shown in Fig. 5 and the free energy profiles for the reaction in the gas phase and aqueous solution are presented in Fig. 6. The reaction has two distinguishable steps.

(1) An intramolecular proton transfer concerted with oxygen alignment (O2, Fig. 5) towards the carbonyl centre forming transition state 1 (TS1) and then a neutral and planar intermediate (minima in the potential energy surface), with a tetragonal sp^3 carbon (C1).

(2) The second step is dehydration, through transition state 2 (TS2), yielding a complex between water and 1,8-An. Both transition states were characterised by a single imaginary frequency and IRC calculations pointed to the expected previous and forward minima structures in the reaction pathway.

Discussion

The pH effect on the observed rate constants for anhydride solvolysis, k_ψ, has been studied in few cases.

The value of k_ψ for decomposition of maleic anhydride derivatives in aqueous solution is pH dependent between pH 3.0 and 5.0 and, since the reactions were followed only up to 0.2 M HCl, additional acid catalysis was not observed.[9] The k_ψ *vs.* pH profile for the dimethylmaleic acid reaction is similar to that obtained here with 1,8-An from pH 1.0 to 6.0. Maleic acid derivatives cyclize only upon protonation of both carboxylic groups.[9]

Spontaneous formation of 1,8-An from 1,8-Acid has been suggested previously.[29,30] We have shown that in the pH 2.0–5.0 region the equilibrium formation of 1,8-An can be adequately described by cyclization of AH_2. Below pH 1.0 the values of 1,8-Acid cyclization rate constants increased sharply with a_{H^+}.

The pH dependence of k_ψ for the anhydride–acid equilibrium was adequately fitted with the equilibria presented in Scheme 3. It should be noted that the equilibrium constant for anhydride formation determined experimentally is identical, within experimental error, to that calculated from the rate constants presented in Table 2 in the pH 1–5 range. This calculation was made possible since the rate constant for water attack on anhydride, k_{-1}, was obtained experimentally (Table 2). Such a comparison was not possible at the higher acidity range since the rate constant for the water attack on the anhydride, k_{-2}, may contain a term in protonated water. Furthermore the error in the estimation of the equilibrium constant at high acidity, K_{E0}, is much larger, since there is essentially total conversion of 1,8-Acid to 1,8-An.

There is extensive literature concerning hydrolysis of anhydrides in aqueous acid.[27,30–33] The effect of high acid concentration (0.5–4 M) on reaction rate is dependent on the structure of the anhydride.[31] Perchloric acid in dioxan–water (60 : 40) increases the hydrolysis rate of glutaric, homophthalic and camphoric anhydrides but inhibits the hydrolysis of maleic and phthalic anhydrides. Univalent salts retard the acid hydrolysis of these cyclic anhydrides. Therefore, for both mono- and bi-cyclic anhydrides there is a relationship between sensitivity to acid, size and configuration of the anhydride ring. However, flexibility of the anhydride ring systems does not affect the sensitivity to acid, *e.g.*, camphoric anhydride has a rigid structure, but nonetheless, its hydrolysis is acid-catalysed. Bunton *et al.* suggested that the acid hydrolysis occurs by an A-2 mechanism involving protonation of an oxygen atom and nucleophilic attack upon the carbonyl carbon atom.[31]

Leisten, in a cryoscopic study of the equilibrium between cyclic anhydrides and diacid in 100% sulfuric acid, suggests that there is an equilibrium between the anhydride and the protonated form of the diacid.[26] This suggestion is in agreement with the protonation proposed in this work for 1,8-Acid below pH 1.0

Anhydride formation from carboxylic acids is a general phenomenon. The equilibrium constant between monocarboxylic acids and its anhydrides lies strongly toward the acid. Acetic acid, for example, at the boiling point, contains only *ca.* 0.03% of the anhydride.[7,8,12] For dicarboxylic acids the equilibrium constant for anhydride formation, K_E, varies from 25 to 1×10^{-5} depending on structure.[12] Apparently, high K_E values for anhydride formation are related mainly to strong non-bonded interactions in the diacid that are relieved in the cyclic anhydride.[12]

Dicarboxylic anhydrides also form in solution upon monoester hydrolysis. Monoesters of dicarboxylic acids hydrolyse by intramolecular nucleophilic attack by the carboxylate ion upon the ester carbonyl yielding anhydrides.[34–37] Linear correlations between the rate constant for diacid cyclization and ΔpK ($pK_{a1} - pK_{a2}$), have been described. The ΔpK of a diacid is largely determined by the existence of an intramolecular hydrogen bonded species in the monoanion. In a study of pK_a of 1,2 dicarboxylic acids attached to rigid skeletons intramolecular hydrogen bonding increases with the distance between the carboxy groups. The stronger intramolecular hydrogen bonding occurs in the monoanion in solution when the carboxy group is spaced so that an essentially linear bond of about 2.45 Å lying

in the intersection of the two planes of the carboxy groups is formed. The carboxy groups should be attached to a carbon skeleton such that no change in conformation of the carbon skeleton is allowed, but the carboxy group may rotate.[22]

The pK_{a1}/pK_{a2} ratios of 1,8- and 2,3-Acid were *ca.* 1.6, implying an intramolecular bonding of the same effectiveness. However, 1,8-Acid cyclizes at pH's below 4.0 while the 2,3-Acid does not cyclize, to a measurable extent, even at 50 °C and 6.0 M HCl. The cyclization of 2,3-Acid cannot be observed using our methods, probably because the equilibrium strongly favours the acid. Hence, the correlation between ΔpK and anhydride formation does not hold for the comparison between 2,3-Acid and 1,8-Acid. In fact, although correlations between ΔpK and rates of anhydride formation do exist in a limited series of diacids, they cannot hold for all diacids.[38] In order for a diacid to exhibit a high ΔpK its geometry should allow the formation of an internal hydrogen bond of about 2.40 Å with little change in molecular strain on going from the open chain to the cyclic form. If, on the other hand, the hydrogen bond in the monoanion is formed at the expense of a large increase in strain, the ΔpK of the diacid may be small. Thus, an important requirement for fast cyclization, apart from the existence of steric strain in the diacid, appears to be that the carboxy groups are as closely situated as possible.[12]

It has been suggested that strain is released in the intramolecular diacid to anhydride conversion.[34] As seen from the calculated structures (see Fig. 5), 1,8-Acid is a rigid and highly strained system, where each carboxy group lies in an opposite side of the aromatic ring plane. On the other hand, the 1,8-An is a rigid but planar structure, without any carboxy interaction resulting in strain.[10,12,13] It was suggested previously that the carboxy group proximity is also determinant in anhydride formation.[12,35–38] Here, and in other bridged cyclic anhydrides where the equilibrium constant for anhydride formation is relatively high, 3 carbon atoms and the anhydride bonds, forming a 6-membered ring, separate both carboxy groups.[13,39] The distance between the attacking oxygen (O2) and electrophilic carbon (C1) is just 2.76 Å in the 1,8-Acid, reaching 2.27 Å in TS1 (Fig. 5). As in similar dicarboxylic acids, strain release and carboxy group proximity are the major factors governing the rate of anhydride formation from 1,8-Acid. The structures 1,8-Acid (see Fig. 5, A) and TS1 (B) are quite different and the pathway could include a previous proton transfer from one oxygen to the other in the same carboxy group. Additional calculations would be necessary to fully investigate this putative step. We can assume, however, that this step may be unimportant kinetically. If such a transfer is not a barrierless process, it would have a smaller energy barrier than a hydrogen transfer between different carboxy groups and, because of short transfer distance, hydrogen tunnelling effects would be present.

The mechanism here proposed for the cyclization of the diprotonated 1,8-Acid is similar to those described where the reaction of a neutral diacid proceeds towards an intramolecular carboxylate attack upon the other carboxy function with final anhydride formation.[35–38]

The K_{E1} value obtained with 1,8-An at 50 °C (see results) agrees reasonably well with the calculated free energy difference between reactant and products (see Fig. 6). Although both the calculated and experimental results are in the range obtained for other similar systems, our purpose with the calculations was not to theoretically obtain the value of the experimental rate constants. Using a simplified model (PCM) to describe solvation effects does not account for specific solvent–solute interactions (*e.g.* hydrogen bonds) that are certainly important in this particular reaction in aqueous solution. Theoretical calculations for cyclization involving a number of explicit water molecules, although possible, was not the subject of our present interest.

Bruice and Lightstone[40] have recently described theoretically a one step intramolecular cyclization reaction with anionic reactants in the gas phase and obtained good agreement with relative rate constants measured in solution. No such series of rate constants is available for the present system. Nonetheless, the calculated mechanism (Figs. 5 and 6) is a possible pathway for the 1,8-Acid cyclization reaction and shows the same proximity and strain features present in the reaction studies of Bruice and Lightstone[40] which account for reaction rate enhancements.

Hawkins'[11] studies of the hydrolysis of phthalic, PTAn, and 3,6-dimethylphthalic, DMPAn, anhydrides show that in aqueous acid DMPAn is in equilibrium with 3,6-dimethylphthalic acid, DMPAcid, while PTAn is quantitatively hydrolysed to phthalic acid, PTAcid, and the equilibrium constant cannot be measured. In water PTAn hydrolyses *ca.* 8 times faster than DMPAn and the cyclization step is *ca.* 6 times faster for DMPAcid. The slower hydrolysis rate of DMPAn is probably not due to steric hindrance towards water attack, but to the relief of steric strain by the methyl groups of DMPAcid, when compared with the corresponding anhydride. Comparison of the thermodynamic parameters for the cyclization reaction for 1,8-Acid and DMPAcid (Table 3) shows that the difference in equilibrium constants reflects differences in the enthalpy term for the equilibrium and not an entropic difference as has been suggested in related systems.[40]

Conclusions

Reversible 1,8-An formation from 1,8-Acid was observed in acidified aqueous solution below pH 5.0 while the decomposition of 2,3-An leads to quantitative formation of 2,3-Acid. The undissociated 1,8-Acid, AH_2, as well as the protonated form, AH_3^+, were the kinetically reactive species. The values of the equilibrium constant for 1,8-An formation of *ca.* 4 and 100, respectively, for the AH_2 and AH_3^+ forms, indicated that protonation stabilizes the anhydride relative to the dicarboxylic acid. *Ab initio* calculations demonstrated that the pathway for anhydride formation includes a rate determining intramolecular proton transfer concerted with oxygen alignment towards the carbonyl centre.

Acknowledgements

The authors are grateful to the Brazilian Agencies FAPESP, CNPq, and CAPES for financial support. This work is part of the MSc dissertation of T.C.B, IQUSP (1991) and of the PhD thesis of S.Y., UFSC (1996). T.C.B. was a CAPES graduate fellow and S.Y. was a CNPq and CAPES fellow. G.M. and L.G.D. are graduate and post-doctoral fellows from FAPESP. The authors thank Dr Jorge Masini, IQUSP, for his helpful suggestions and for his computational advice in the calculation of potentiometric pK_a's of the diacids and Professor C. A. Bunton, UCSB, USA, for advice and helpful suggestions with the manuscript.

References

1 A. J. Kirby, *Adv. Phys. Org. Chem.*, 1980, **17**, 183.
2 W. P. Jencks, *Catalysis in Chemistry and Enzymology*, Dover, New York, 1987.
3 S. Y. Yunes, J. C. Gesser, H. Chaimovich and F. Nome, *J. Phys. Org. Chem.*, 1997, **10**, 461.
4 T. C. Barros, *Formação e Decomposição de Naftalimidas em Solução Aquosa: Dependência Estrutural e Efeito de Micelas*, Masters Thesis, Chemistry Institute, Biochemical Department, University of São Paulo, USP, São Paulo, Brazil, 1991.
5 S. F. Yunes, *Hidrólise de Monoalquil Ésteres do Ácido 1,8-Naftálico*, PhD Thesis, Department of Chemistry, Centro de Ciências F´sicase Matemáticas, Universidade Federal de Santa Catarina, UFSC, Florianópolis, Santa Catarina, Brazil, 1996.
6 M. Bender, *Chem. Rev.*, 1960, **60**, 53.
7 J. A. Knopp, W. S. Linnell and W. C. Child, Jr., *J. Phys. Chem.*, 1966, **66**, 1513.

8 W. P. Jencks, F. Barley, R. Barnett and M. Gilchrist, *J. Am. Chem. Soc.*, 1966, **88**, 4464.
9 L. Eberson, *Acta Chem. Scand.*, 1964, **18**, 1276.
10 T. Higuchi, L. Eberson and J. D. McRae, *J. Am. Chem. Soc.*, 1967, **89**, 3001.
11 M. D. Hawkins, *J. Chem. Soc., Perkin Trans. 2*, 1975, 282.
12 L. Eberson and H. Welinder, *J. Am. Chem. Soc.*, 1971, **93**, 5821.
13 L. Eberson and L. Landstrom, *Acta Chem. Scand.*, 1972, 239.
14 A. D. Campbell and M. R. Grimett, *Aust. J. Chem.*, 1963, **16**, 854.
15 R. H. Boyd in *Solute Solvent Interactions*, Ed. J. F. Coetzee and C. D. Ritchie, 1969, Marcel Dekker, New York.
16 D. A. MacQuarrie, *Statistical Mechanics*, Harper & Row, New York, 1976.
17 K. Fukui, *Acc. Chem. Res.*, 1981, **14**, 363.
18 C. Gonzales and B. H. Schlegel, *J. Phys. Chem.*, 1990, **94**, 5523.
19 J. Tomasi and J. Pérsico, *Chem. Rev.*, 1994, **94**, 2027.
20 M. J. Frisch, G. W. Trucks, H. B. Schlegel, G. E. Scuseria, M. A. Robb, J. R. Cheeseman, V. G. Zakrzewski, J. A. Montgomery, Jr., R. E. Stratmann, J. C. Burant, S. Dapprich, J. M. Millam, A. D. Daniels, K. N. Kudin, M. C. Strain, O. Farkas, J. Tomasi, V. Barone, M. Cossi, R. Cammi, B. Mennucci, C. Pomelli, C. Adamo, S. Clifford, J. Ochterski, G. A. Petersson, P. Y. Ayala, Q. Cui, K. Morokuma, D. K. Malick, A. D. Rabuck, K. Raghavachari, J. B. Foresman, J. Cioslowski, J. V. Ortiz, B. B. Stefanov, G. Liu, A. Liashenko, P. Piskorz, I. Komaromi, R. Gomperts, R. L. Martin, D. J. Fox, T. Keith, M. A. Al-Laham, C. Y. Peng, A. Nanayakkara, C. Gonzalez, M. Challacombe, P. M. W. Gill, B. Johnson, W. Chen, M. W. Wong, J. L. Andres, C. Gonzalez, M. Head-Gordon, E. S. Replogl and J. A. Pople, *Gaussian 98, Revision A.6*, Gaussian, Inc., Pittsburgh PA, 1998.
21 J. C. Masini, *Talanta*, 1994, **41**, 1383.
22 L. L. McCoy, *J. Am. Chem. Soc.*, 1967, **89**, 1673.
23 T. C. Barros, G. R. Molinari, P. Berci-Filho, V. G. Toscano and M. J. Politi, *J. Photochem. Photobiol.*, 1993, **76**, 55.
24 R. P. Bell, *The Proton Chemistry*, 2nd edn., 1973, Chapman and Hall, London, UK.
25 L. P. Hammett, *Physical Organic Chemistry*, 1970, 2nd edn., McGraw-Hill Kogakusha, Japan.
26 J. A. Leisten, *J. Chem Soc.*, 1961, 2191.
27 C. A. Bunton, J. H. Fendler, N. A. Fuller, S. Perry and J. Rocek, *J. Chem. Soc.*, 1965, 6174.
28 *CRC Handbook of Chemistry and Physics*, ed. R. C. Weast, 52nd edn., 1971, The Chemical Rubber Co., USA.
29 L. J. Fitzgerald, R. E. Gerkin and G. D. Renkes, *Vib. Spectrosc.*, 1991, **2**, 269.
30 R. Aroca, S. Corrent and J. R. Menendez, *Vib. Spectrosc.*, 1997, **13**, 221.
31 C. A. Bunton, J. H. Fendler, N. A. Fuller, S. Perry and J. Rocek, *J. Chem. Soc.*, 1963, 5361.
32 C. A. Bunton, N. A. Fuller, S. Perry and V. J. Shiner, *J. Chem. Soc.*, 1963, 2918.
33 C. A. Bunton, N. A. Fuller, S. Perry and I. H. Pitman, *J. Chem. Soc.*, 1962, 4478.
34 E. Gaetjens and H. Morawetz, *J. Am. Chem. Soc.*, 1960, **82**, 5328.
35 T. C. Bruice and U. K. Pandit, *J. Am. Chem. Soc.*, 1960, **82**, 5858.
36 T. C. Bruice and U. K. Pandit, *Proc. Natl. Acad. Sci. USA*, 1960, **46**, 402.
37 T. C. Bruice and W. C. Bradbury, *J. Am. Chem. Soc.*, 1965, **87**, 4846.
38 T. C. Bruice and W. C. Bradbury, *J. Am. Chem. Soc.*, 1965, **87**, 4851.
39 H. K. Hall, Jr., *J. Org. Chem.*, 1963, **28**, 2027.
40 T. C. Bruice and F. C. Lightstone, *Acc. Chem. Res.*, 1999, **32**, 127.